This is a preprint of an article published in the Information Sciences journal, ISSN 0020-0255.
Please see the final version at: https://doi.org/10.1016/j.ins.2021.08.011

Ensemble ellipse fitting by spatial median consensus

Karl Thurnhofer-Hemsi[a,*], Ezequiel López-Rubio[a], Elidia Beatriz Blázquez-Parra[b], M. Carmen Ladrón-de-Guevara-Muñoz[b], Óscar David de-Cózar-Macías[b]

[a] *Department of Computer Languages and Computer Science, University of Málaga, Bulevar Louis Pasteur, 35, 29071, Málaga, Spain*
Biomedic Research Institute of Málaga (IBIMA), C/ Doctor Miguel Díaz Recio, 28, 29010, Málaga, Spain

[b] *Department of Graphical Engineering, Design and Projects, University of Málaga, C/ Doctor Ortiz Ramos, 29071, Málaga, Spain*

Abstract

Ellipses are among the most frequently used geometric models in visual pattern recognition and digital image analysis. This work aims to combine the outputs of an ensemble of ellipse fitting methods, so that the deleterious effect of suboptimal fits is alleviated. Therefore, the accuracy of the combined ellipse fit is higher than the accuracy of the individual methods. Three characterizations of the ellipse have been considered by different researchers: algebraic, geometric, and natural. In this paper, the natural characterization has been employed in our method due to its superior performance. Furthermore, five ellipse fitting methods have been chosen to be combined by the proposed consensus method. The experiments include comparisons of our proposal with the original methods and additional ones. Several tests with synthetic and bitmap image datasets demonstrate its great potential with noisy data and the presence of occlusion. The proposed consensus algorithm is the only one that ranks among the first positions for all the tests that were carried out. This demonstrates the suitability of our proposal for practical applications with high occlusion or noise.

Keywords: ellipse fitting, conic fitting, ensemble methods, L1-norm, spatial

*Corresponding author
Email address: karlkhader@lcc.uma.es (Karl Thurnhofer-Hemsi)
URL: http://www.lcc.uma.es/\%7Eezeqlr/index-en.html (Ezequiel López-Rubio)

1. Introduction

Nowadays, it is well known that fitting geometric primitive models is a fundamental task in pattern recognition, computer vision, and even in digital image analysis. There is a wide range of geometric primitives available, including piecewise polynomial curves and surfaces [2, 44], and analytic curves such as the circle, the parabola, or the ellipse [28]. This last one has a great significance in computer graphics, metrology, industrial procedures, and other applications [45, 48]. Some illustrations of the ellipse fitting methods importance have been researched. One example is eye localization that it is needed for face recognition, device interaction, or face alignment. Regarding industrial environments, another subject is camera calibration based on ellipses fitting since the projection of cylinders are used to determine the camera position and orientation. In other application fields such as biology, chemistry, and nanotechnology, ellipses fitting is also used. Li [26] shows a reliable, effective, and accurate approach to this type of problems, for instance, on the subject of handprints identification. As an example of the variety of applications, Islam et al. [20] introduce an ellipse fitting method in vascular permeability images used for non-invasive procedures, which are relevant for monitoring cancer solid tumors based on the use of ultrasound poroelastography.

Two categories of fitting problems could be distinguished, depending on whether they are based on algebraic or geometric fitting [14, 33]. Both are differentiated by their error distance definition.

Thus, in an algebraic fitting, the curve is given by a constrained implicit equation of a conic. This fitting has implementation and computational cost advantages [33], but also some drawbacks such as accuracy, physical interpretation of the fitting parameters, errors, and sensitivity to outliers. Although the algorithms are efficient, the solution is not always an ellipse.

Nevertheless, several kinds of research have been working on least-squares problems based upon the square of the sum of algebraic distances or its variations, [14, 21, 41]. As reported by Ahn et al. [1], there were some fit drawbacks that have been resolved by other authors. Therefore, the Direct Least Square method was one of the significant advances in algebraic procedures suggested by Fitzgibbon et al. [14]. A new computationally efficient constraint was their contribution, which guaranteed that an ellipse was the optimal solution. On the other hand, Ahn et al. [1] used the Orthogonal Least Squares Fitting, introducing some enhancements that overcame the weak points of this fitting scheme. They try to minimize the sum of the orthogonal distances. This criterion has a clear geometric understanding because the Euclidean distance from the points is used as an error measure to solve the issue. However, it must be solved iteratively.

The geometric distance is employed by many researchers using a function of elliptical parameters; in other words, the "Sampson error" [33, 41]. Kanatani [21] proposed a renormalization, while Chojnacki et al. [9] a Fundamental Numerical Scheme (FNS) or Leedan and Meer [25] and Matei and Meer [29] Heteroscedastic Errors in Variable (HEIV). Kanatani and Sugaya [22] have proved that the Sampson error shows an excellent estimation of the geometric distance, and its minimization outcome is close to the true geometric fit. Meanwhile, Calafiore [8] presents a fitting solution for a set of points in reference to the difference of squares geometric error model. The proposed algorithms are based on a closed-form solution that guarantees a global minimum is reached in a limited amount of iterations.

Genetic algorithms have been used by Fraga et al. [10] and Ray et al. [37] to solve optimization problems of ellipse fitting. The purpose is to minimize the sum of orthogonal Euclidean distances from the given points. Roth and Levine [39] applied the Least Median of Squares as a robust estimator, and it has been contrasted to other robust processes such as Rosin [38]. On the other hand, Yu et al. [47] determined a new geometric objective function considering that the sum of the distances from the point to the foci is constant. Finally, Muñoz et al. [33] used the criteria in reliance on the least mean absolute geometric error considering that the optimum value of the sum of distances from the points to the foci is computed by using the median, a robust estimator. This method detects the presence of outliers [30]. Consequently, other methods like RANSAC [7] shown by Fischler and Bolles were not necessary.

Ellipse fitting is a challenging task because outlying input samples can easily undermine the quality of the fit. Robustness is often achieved in other estimation tasks by averaging several fits. However, ellipse fits are difficult to merge because simple averaging schemes for the ellipse parameters yield poor results. This means that the development of specific and adequate averaging methods for ellipse fitting is crucial to the success of ensemble strategies. In this work, a proposal of this kind is presented.

Our proposed method tries to combine the best ellipse fitting algorithms using a consensus criterion. This is done by converting the outputs of the original methods to a natural parametrization that is amenable to averaging. After that, the spatial median (also called L1 median) is employed to obtain accurate estimates of the true ellipse. This way, the defects of the outputs of the individual methods for specific input datasets are smoothed out by the spatial median calculation. Therefore, the main contributions of this work are:

- The proposal of the natural parametrization of the ellipse to combine different ellipse fits, since the natural parametrization attains a better quality of the combined fits.

- The selection of five ellipse fitting methods to serve as the basis of a consensus.

- The usage of the spatial median in order to combine the natural parameters of the ellipse fits coming from the five base methods.

The rest of the paper has the following structure. Firstly, Section 2 summarizes previous ellipse fitting techniques used in the applied consensus. Secondly, the mathematical background of our proposal is described in Section 3. Then, the results of the different experiments carried out are reported in Section 4. To conclude, the findings of this work are related in Section 5.

2. Previous work

Some decision-making problems can be solved by using the consensus procedure [27, 35, 46]. It is important to clarify that a logical consensus method is not only a set or collection of viewpoints, but a way where rational consensus changes are due to individual preferences. The consensus word is described as an interactive and constant decision change procedure managed by a coordinator or moderator. This person performs several tasks such as having a main role in the decision making, supplying back information, and making suggestions to the decision-makers in order to advance to a determined consensus level. The moderator establishes the most appropriate consensus model and decides a set of parameters for the selected model. A review of fuzzy consensus models has been provided by Cabrerizo et al. [5] and Herrera-Viedma et al. [18]. Lately, researchers have introduced new models founded on iterations based approaches [3] and on optimizations based approaches [13]. Previously to the consensus procedures, only a low number of decision-makers were considered. Nevertheless, the economy and technology evolution has enhanced the organizations' demand, i.e., e-democracy and social networks, emergency management, and teacher appointment reformation system at universities. Currently, in the wide-scale collective decision-maker problems, the number of decision-makers has raised from a few to thousands. Due to the vast diversity of backgrounds and diverse resources and information, it is even more challenging to reach an agreement among the participators for common group decision problems.

Ensemble classifiers [4, 32] combine individual opinions from homogeneous and heterogeneous models; thereby, the generalization ability is improved, and the overfitting risk is reduced [24]. Dietterich [11] ensures that a single classifier is worse than an ensemble for the following reasons. First, accounting on a single classifier is not ideal, as it could be badly chosen. Secondly, local search is used by some learning algorithms, so it might not find the optimal model.

In this case, running the learning algorithm several times and combining the achieved models concludes that this approximation as an optimal classifier is better than any single one. Eventually, the optimal model may be obtained by combining different classifiers since the optimal function is not usually reached by machine learning problems. In fields as medicine, bioinformatics, finance, recommender systems, and image retrieval, the ensemble classifiers have been successfully used.

The following ellipse fitting methods have been considered in this work:

- Taubin method [43]: a non-iterative curve fitting method based on its implicit representation to a dataset minimizing the approach mean square distance, which is a non-linear least squares problem. It could fit different types of curves: hyperbola, ellipse, parabola, and others. This method was derived by Taubin (1991) heuristically without considering the statistical properties of the noise.

- Szpak method [42]: an ellipse estimation procedure is introduced, supported on optimization of the Sampson distance as a quality measure between the estimated ellipse and the dataset. This Sampson distance optimization is achieved with a particular alternative to the Levenberg-Marquardt algorithm.

- Fitzgibbon method [15, 47]: an efficient method that minimizes the algebraic distance and incorporates the ellipticity constraint into the normalization factor to fit an ellipse. This constraint guarantees that the result is a real ellipse rather than a general conic feature and also avoids the parameter-free scaling problem.

- PARE method: it is a geometric ellipse fit loop that computes the best fit ellipse in parameter form to a group of given points. The procedure is tested among the following optimization techniques as Gauss-Newton with Marquardt, Newton with Marquardt, Marquardt and Gauss-Newton.

- Muñoz method [33]: it is a robust multicriteria algorithm that considers the eccentricity and the geometric features of the data points to fit an ellipse based on the mean absolute error.

- Halir&Flusser method [17]: a numerically stable non-iterative approach based on a least squares minimization. It is a simple and direct fitting method that always provides a fit even for very noisy data, making it useful for an initial robust ellipse estimation that can be fed into a more complex ellipse fitting method.

- Rosin method ($A+C=1$) [38]: the least median of squares method is used as the most appropriate procedure in terms of robustness and accuracy. The geometric parameters are estimated as the median of the parameters of the speculated ellipses.

- Prasad method [36]: this work proposes a least squares ellipse fitting method without the requirement of any constrained optimization. This method uses the ellipses actual parameters in a non-linear manner. Therefore, the proposed non-iterative technique is numerically and computationally efficient, being very stable against high levels of noise.

In the next section, our proposed ensemble ellipse fitting method is presented.

3. The method

Our aim is to combine several ellipse fitting methods in a reliable way, so that large deviations from the correct solution by some methods of the ensemble do not substantially affect the consensus solution, provided that the majority of the combined methods still produce acceptable solutions.

Let $\boldsymbol{\theta} \in \mathbb{R}^D$ be a characterization of the ellipse, where D is the number of characterization parameters. For an ellipse $D \geq 5$, since the ellipse has five degrees of freedom. Also, let N be the number of training samples available for the ellipse fitting methods, and $\mathcal{T}$ the training set:

$$\mathcal{T} = \left\{ (x_i, y_i) \in \mathbb{R}^2 \mid i \in \{1, ..., N\} \right\} \tag{1}$$

where (x_i, y_i) are the coordinates of the i-th training sample in the two dimensional plane.

Finally, let M be the number of ellipse fitting methods in the ensemble, so that the j-th method in the ensemble generates a solution $\tilde{\boldsymbol{\theta}}_j \in \mathbb{R}^D$ for a given training set $\mathcal{T}$, where $j \in \{1, ..., M\}$.

In order to combine the solutions generated by multiple methods, the correct solution can be approximated by the expectation $\hat{\boldsymbol{\theta}}$ of those solutions:

$$\hat{\boldsymbol{\theta}} = \mathbb{E}\left[\tilde{\boldsymbol{\theta}}\right] \tag{2}$$

where $\mathbb{E}$ stands for the mathematical expectation operator. One could try to estimate $\hat{\boldsymbol{\theta}}$ by the sample mean:

$$\bar{\boldsymbol{\theta}}_{L2} = \frac{1}{M}\sum_{j=1}^{M} \tilde{\boldsymbol{\theta}}_j \tag{3}$$

This strategy would minimize the sum of L2-norms of the residuals, i.e. the squared Euclidean distances:

$$\bar{\boldsymbol{\theta}}_{L2} = \arg\min_{\boldsymbol{\theta}\in\mathbb{R}^D} \sum_{j=1}^{M} \left\|\boldsymbol{\theta} - \tilde{\boldsymbol{\theta}}_j\right\|^2 \tag{4}$$

where $\|\cdot\|$ stands for the Euclidean distance.

Minimization of L2-norms might lead to a poor estimation of the ellipse, since any single sample $\tilde{\boldsymbol{\theta}}_j$ with a large error with respect to the true solution will completely ruin the estimation. Therefore we propose to minimize the sum of the Euclidean distances:

$$\bar{\boldsymbol{\theta}}_{L1} = \arg\min_{\boldsymbol{\theta}\in\mathbb{R}^D} \sum_{j=1}^{M} \left\|\boldsymbol{\theta} - \tilde{\boldsymbol{\theta}}_j\right\| \tag{5}$$

This is also known as the spatial median or L1 median [23, 31, 34] of the solution set $\mathcal{S}$:

$$\mathcal{S} = \left\{\tilde{\boldsymbol{\theta}}_j \in \mathbb{R}^D \mid j \in \{1, ..., M\}\right\} \tag{6}$$

There are several algorithms to compute the L1 median of a set. Here, the method described in [19] has been selected due to its accuracy and speed.

In order to fully specify the proposed method, a characterization of the ellipse must be chosen. Three characterizations of the ellipse have been considered: algebraic, geometric and natural. Next, their suitability for our purposes is analyzed.

The algebraic characterization of the ellipse is given by a vector of six algebraic parameters:

$$\boldsymbol{\theta}_{algebraic} = (A, B, C, D, E, F) \tag{7}$$

The six algebraic parameters are associated to the general equation of a conic section:

$$Ax^2 + Bxy + Cy^2 + 2Dx + 2Ey + F = 0 \tag{8}$$

The algebraic characterization of the ellipse is not amenable to our purposes for two reasons. First of all, it is not normalized, i.e. there can be many algebraic parameter vectors which correspond to the same ellipse. This can be fixed by fixing $A + C = 1$, for example. However, there is a more serious inconvenient, namely the fact that the consensus of several ellipses by (5) might not correspond to an ellipse, since the algebraic parametrization can also represent other conic sections. Therefore, the algebraic parametrization is not adequate to ensure that the consensus result is an ellipse.

The geometric characterization considers the following parameter vector:

$$\boldsymbol{\theta}_{geometric} = (\bar{x}, \bar{y}, a, b, \varphi) \tag{9}$$

where $(\bar{x}, \bar{y}) \in \mathbb{R}^2$ is the center of the ellipse, a is the half length of the major axis, b is the half length of the minor axis, $a \geq b > 0$, and $\varphi \in [0, \pi]$ is the angle of tilt. The main difficulty of this parametrization is that averaging the angles φ might lead to extraneous solutions, in particular for values of the angle close to the interval limits 0 and π.

A different kind of geometric parametrization, hereafter called the natural parametrization, is defined as follows:

$$\boldsymbol{\theta}_{natural} = (f_{x1}, f_{y1}, f_{x2}, f_{y2}, s) \tag{10}$$

where $(f_{x1}, f_{y1}) \in \mathbb{R}^2$ is the first focus of the ellipse, $(f_{x2}, f_{y2}) \in \mathbb{R}^2$ is the second focus of the ellipse, and $s > 0$ is the sum of distances to both foci of the points that lie in the ellipse, $s = 2a$. The natural parametrization has some crucial advantages over the previous ones:

- As opposed to the algebraic parametrization, the consensus by (5) of any number of solutions always results in an ellipse.
- As opposed to the geometric parametrization, there is no angle averaging, so extraneous consensus solutions are avoided.
- The five parameters are distances measured on the plane where the samples lie, so that the scales of the parameters are the same. Furthermore, Eq. (5) can be interpreted as the computation of the L1 median of a set of points in $\mathbb{R}^5$, where all five dimensions have the same importance because their scales are the same.

Given the above considerations, the natural parametrization is proposed to be used for our method.

So as to establish the consensus algorithm, the following $M = 5$ methods of ellipse fitting from the literature were selected: Taubin, Fitzgibbon, PARE, Muñoz, and Szpak. When some of the previous algorithms are not able to achieve a fit of the ellipse, then they are not considered into the consensus. As an emergency backup solution whenever the consensus cannot be computed, Muñoz method is employed as our algorithm's solution because it is the most stable.

4. Experimental Results and Discussion

This section collects a set of experiments applied to different kinds of datasets. In Subsection 4.1, the performance measures used for comparisons are described. Secondly, the description and results of experiments with synthetic data are reported in Subsection 4.2. Finally, Subsection 4.3 depicts examples of applying the method with bitmap image data.

The proposed method[1] have been compared to the five methods that are combined in our consensus algorithm, i.e., Taubin, Szpak, Fitzgibbon, PARE, and Muñoz. In addition to this, it has been compared with Halir&Flusser, Rosin, and Prasad, methods described in Section 2. The recommended default parameters for each method were used to carry out a fair comparison among all of them. The PARE method was used with Gauss-Newton and Marquardt fitting algorithm and parameter initialization by Fitzgibbon. Prasad method needed a rescale of the dataset to work well, so a scale-up value of 100 was used, and the geometric parameters of the fitted ellipse were scaled down then.

4.1. Evaluation metrics

Firstly, the evaluation of the results was carried out using four different measures:

- The error of the natural parameters of the ellipse (ParNError. When the algorithm fits an ellipse, the natural parameters (10) are computed and they are compared with the parameters of the true ellipse (if it is available) as

$$ParNError = \sqrt{\sum_{i=1}^{5}(\boldsymbol{\theta}^{i}_{true\_natural} - \boldsymbol{\theta}^{i}_{est\_natural})^2} \tag{11}$$

- The Root Mean Square Orthogonal error (RMSOError). It is a geometric error that measures the orthogonal distance d_i [49] between the estimated ellipse and points lying on the true ellipse. A test set of T true points are computed from the true ellipse and then the RMS error using those orthogonal distances is calculated as

$$RMSOError = \sqrt{\frac{1}{T}\sum_{i=1}^{T} d_i^2} \tag{12}$$

  Five points on the true ellipse are manually selected on the image for the purpose of generating the test set. Thus, Eq. (8) is used to solve a

[1] The source code and demos of the proposed method will be published in case of acceptance.

linear system and find the general form of the true ellipse. After that, the geometric parameters are computed in order to generate T points of the true ellipse varying the angle φ.

- The error of the algebraic parameters of the ellipse (ParAError). When the algorithm fits an ellipse, the algebraic parameters (8) are computed and normalized, so they can be compared with the true parameters as follows:

$$ParAError = \sqrt{\sum_{i=1}^{5} \left(\frac{\boldsymbol{\theta}^i_{true\_algebraic}}{||\boldsymbol{\theta}_{true\_algebraic}||} - \frac{\boldsymbol{\theta}^i_{est\_algebraic}}{||\boldsymbol{\theta}_{est\_algebraic}||} \right)^2} \tag{13}$$

- The Euclidean Ellipse Comparison Metric (ECCM). It is a more complex geometric measure, where the average distance between two ellipses is computed using the minimum distance d between a point of one ellipse's contour to another, and vice versa [6], for a set of n points.

$$ECCM = \frac{1}{2n} \sum_{i=1}^{n} \left(d(p_i^{E_1}, E_2) + d(p_i^{E_2}, E_1) \right) \tag{14}$$

In addition to these metrics, the performance evaluation is completed building performance profiles [12] of the set of methods $\mathcal{M}$ on a test set $\mathcal{P}$. If $|\mathcal{M}| = n_m$ and $|\mathcal{P}| = n_p$, for each problem p and solver method m, we define:

$$e_{p,m} = \text{error obtained when problem } p \text{ is solved with method } m$$

where $e_{p,m} \in \{ParNError_{p,m}, RMSOError_{p,m}, ParAError_{p,m}, ECCM_{p,m}\}$. Then, the performance on problem p by method m is compared with the best performance achieved by any solver on this problem defining the ratio:

$$r_{p,m} = \frac{e_{p,m}}{min\{e_{p,m} : m \in \mathcal{M}\}} \tag{15}$$

For those problems where there are methods that cannot fit an ellipse, the correspondent ratio is established to the greatest value of all ratios:

$$r_{MAX} = max\{r_{p,m} : p \in \mathcal{P}, m \in \mathcal{M}\} \tag{16}$$

Finally, a probability cumulative distribution is defined to obtain an overall assessment of the performance of each method:

$$\rho_m(\tau) = \frac{1}{n_p} |\{p \in \mathcal{P} : r_{p,m} \leq \tau\}| \tag{17}$$

Thus, $\rho_m(\tau)$ is the probability that a performance ratio $r_{p,m}$ is within a factor $\tau \in \mathbb{R}$ of the best possible ratio, for a chosen method m. Summarizing, the method that first achieves the maximum probability is the one that solves the highest number of ellipse fitting problems with the smallest error.

4.2. Synthetic data

Firstly, artificially generated data was used in order to evaluate the performance of the method from a quantitative point of view. For each experiment, the center, the major and minor axes and the tilt angle of an ellipse are chosen at random uniformly:

$$c_x, c_y \sim U\left(0, 1\right) \tag{18}$$

$$a \sim U\left(0.2, 1\right) \tag{19}$$

$$b \sim U\left(0.1, 1\right) \tag{20}$$

$$\phi \sim U\left(\frac{-\pi}{2}, \frac{\pi}{2}\right) \tag{21}$$

where U represents the uniform distribution. The major and minor axes (a, b) are selected inside the unit square but in different ranges in order to avoid degenerated ellipses.

Then, sample points $\mathbf{s} \in \mathbb{R}^2$ are uniformly generated on the canonical coordinate system:

$$\mathbf{s} = (a\ b) \cdot \begin{pmatrix} cos\theta & 0 \\ 0 & sin\theta \end{pmatrix} \tag{22}$$

where θ is an angle randomly selected from the uniform distribution $U(\theta_s, \theta_e)$, and $\theta_s, \theta_e \sim U\left(-\pi, \pi\right)$ are the starting and ending angle of the unit canonical system. In order to avoid datasets with too small curvature which lead to

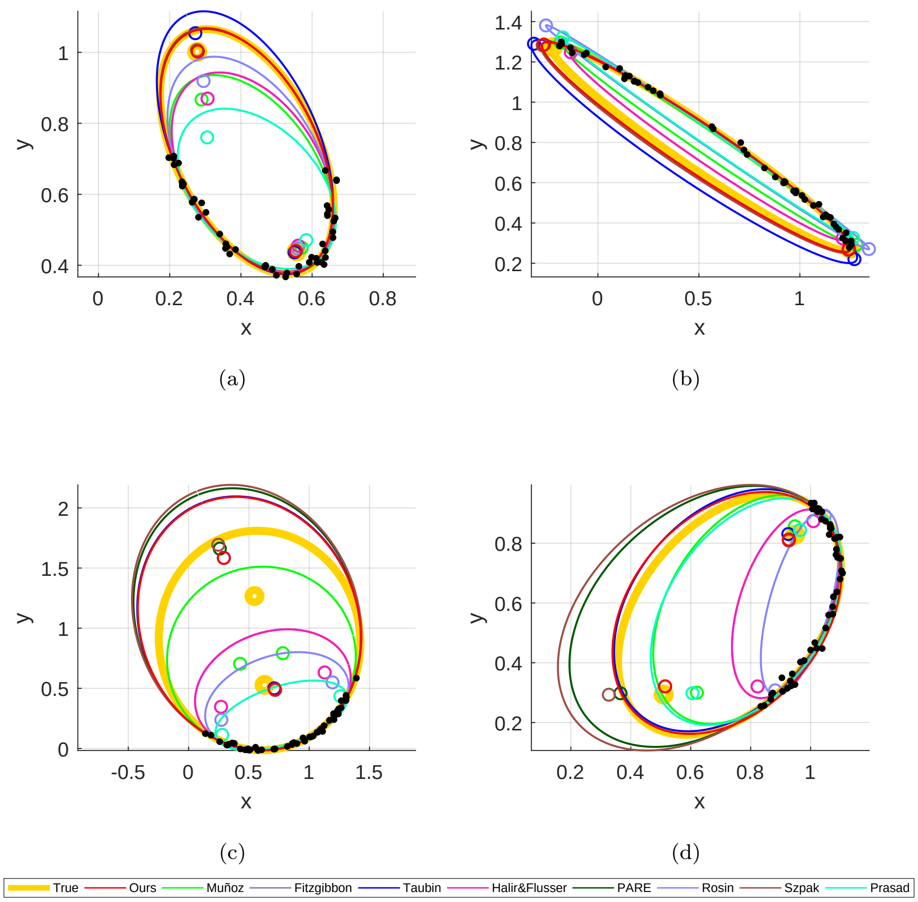

Figure 1: Graphical comparison of the tested methods performance using synthetic data generation. Four different initializations and their solutions are shown. The black points are the training samples. The yellow thick curve represents the true ellipse, while the narrow curves show the outcome of each method.

degenerate solutions, points that are enclosed into an arc larger that 1 radian are chosen, i.e., angles which satisfy that:

$$\theta_e - \theta_s > 1 \tag{23}$$

In the end, 1% of normally distributed Gaussian noise was added to the samples. A total of $N = 50$ input samples were created in order to feed the ellipse fitting methods. For the quantitative comparisons, $T = 1000$ test samples of the true ellipse were generated (without the presence of noise).

Next, Figure 1 presents four different examples of the execution of our consensus method. The true ellipse is plotted with a thick yellow edge. The first example shows a dataset with approximately 50% of occlusion. Our proposal and Rosin methods achieved the best fit, while the rest of the methods only fitted a smaller ellipse, except for Taubin method. Figure 1b exhibits an eccentric ellipse. Although the dataset is very rectilinear, all the algorithms achieve a good adjustment on the samples. There is not a clear winner, but the most accurate method seems to be the proposed one. In the adjustments shown in Figures 1c and 1d more disparity between the methods can be observed. The higher level of occlusion produces ellipses with different orientations in the first case. However, as our method is based on the spatial median computation of the foci and three of the best methods were included in the consensus, it has hardly been affected by wrong fits. Something similar happened in the last case, where there are diverse types of ellipses with different sizes. The median value of the sum of distances to both foci corrects the ellipse and provides an accurate fit.

Figure 2 shows the performance profiles for the 1000 executions. As explained in Subsection 4.1, these graphics show how better one method is with respect to the best one. Hence, the method which first achieves probability one is considered more efficient than the others. For the ParN error, our proposal solves almost 95% of the executions with a better error ratio. The completion of the rest of the executions was reached only by Muñoz and Halir&Flusser methods, along with our proposal, being the best methods in solving all the

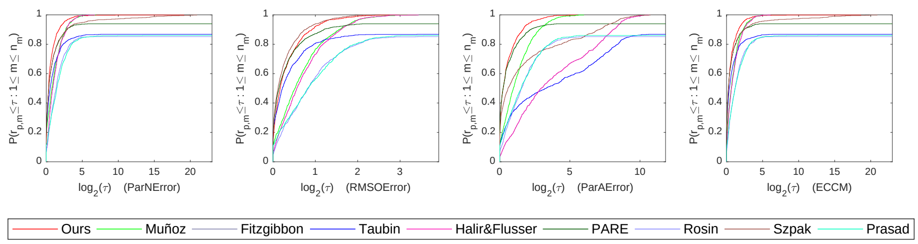

Figure 2: Performance profiles of the synthetic experiments (the closer to the upper left corner, the better) with 1% of Gaussian noise added. ParNError and RMSOError metrics are analyzed. X axis shows the factor of the best possible ratio in a logarithmic scale and Y axis represents the probability cumulative distribution.

fittings. However, Prasad, PARE, and Taubin fail in 10-20% of the fittings, which means that there are several cases where those methods cannot compute an ellipse and generate a different kind of estimations. In terms of RMSO error, Szpak method is the best one followed by our consensus method, with similar behavior until $\sim 92\%$ of executions. Considering both measures, we can see that the best methods for the ParN error are now clearly below the performance of the best methods for the RMSO error, except our proposal, which is stable in the first positions for both error metrics.

4.2.1. Noise analysis

In this subsection the behavior of our method with the presence of higher levels of noise is studied. Gaussian noise of levels 2%, 3%, 4% and 5% was added to the synthetic data and 1000 executions were carried out. Performance profiles for all error measures were computed and results are displayed in Figure 3. Logarithmic scale is used on behalf of clarity.

In terms of the ParN error (first row of Figure 3), our method clearly outperforms all the competing methods, achieving the lowest error ratio for almost all executions. Rosin, PARE, Prasad, and Taubin methods are affected by the noise increment, as they can not solve all the problems, but only between 60-90% of them. Szpak also does not fit all the ellipses appropriately when the noise level rises. However, for its successful fittings ($log_2(\tau) < 2$) the ratio error is one of the best ones, something that contributes to the good performance of our consensus method.

Analyzing the RMSO error in the second row of Figure 3, the excellent performance of Szpak explained above is well represented. This method achieves the best error ratios for almost all the executions, followed by our proposal. Muñoz and Halir&Flusser methods have a similar tendency for all the noise levels; they perform better as the noise is increased, which means that they are also resilient to noise. In the previous figure, the good performance of these algorithms is also shown. However, when $\tau < \sqrt{2}$ they misbehave, they are closer to the worst methods' results, meaning that they are unstable for some fitting problems.

The outcomes of the ParA error, which are shown in the third row of Figure 3, allow us to have a third point of view of the performance of each method. In this case, the PARE method yields good results (especially for 2-3% of noise), although it is not able to complete all the fits. Opposite to what happens with the other measures, the Szpak method generates considerably worse algebraic parameters. Muñoz method has the same tendency as in the previous analysis. All in all, our proposal remains stable, being the best method when the level of noise is higher.

Finally, the ECCM results are presented in the fourth row of Figure 3. Halir&Flusser method obtained outstanding results compared with the other metrics, and together with our proposal, they are the best methods. Also, Muñoz method worked well with lower levels of noise. This measure reflects the geometrical accuracy of the fit, but as it is an average of distances, it does not distinguish between solutions that are very eccentric with both large semiaxes. The good performance of our method in terms of ECCM combined with the other measures reflects that it is more accurate than its competitors for any scenario.

Figure 4 shows a concrete example of the evolution of the fitting for each method. Sample points of a half ellipse are depicted with the addition of 2%, 3%,

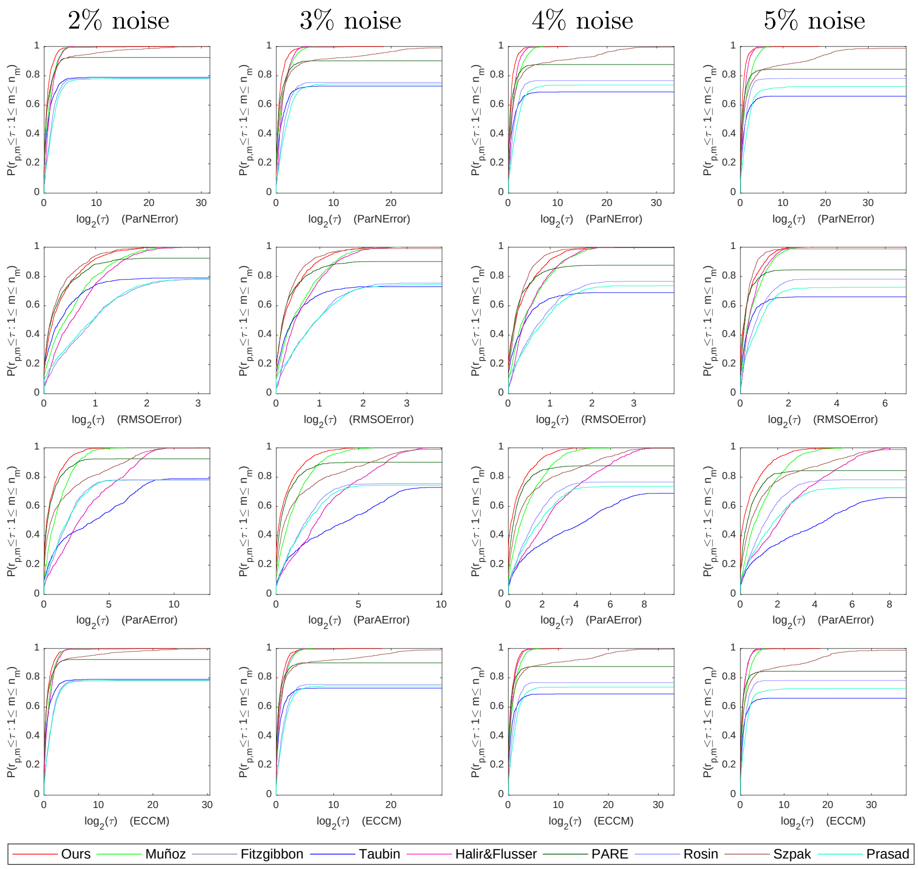

Figure 3: Noise analysis by the performance profiles of synthetic experiments (the closer to the upper left corner, the better). The four error measures are analyzed with 2%, 3%, 4% and 5% of Gaussian noise added. X axis shows the factor of the best possible ratio in a logarithmic scale and Y axis represents the probability cumulative distribution.

4%, and 5% of noise. For the first test shown in Figure 4a, Rosin, Halir&Flusser, and Prasad are the methods that do not achieve the ellipse fitting. The rest of the algorithms obtain a good result. When the noise is lightly increased, Muñoz method also fails in the fitting. In Figures 4c and 4d these methods perform even worse. Focusing on the best ones, we can see that the presence of higher levels of noise also affects the performance of Szpak and Taubin. However, PARE and ours, which are almost overlapped, generate the best ellipse according to the ground truth.

For the sake of clarity, Figure 5 depicts the boxplots of the 1000 runs, with the mean and the median values. As a penalization term, twice the maximum error found was assigned to those uncompleted fits. This procedure is equivalent to the one used by the performance profiles. The methods with the smallest dispersion are Muñoz, PARE, Halir&Flusser, Szpak, and Ours, although the last three seem to be the most competitive in terms of mean and median values. Szpak gives a lot of bad executions, which is noticeable in the ECCM boxplot in the gray dots coming out above its box (the samples that have a substantial error). It must be emphasized that it is a very unreliable estimator. On the other hand, the fact that the mean for the PARE method is worse in most error measures indicates that some PARE executions are very bad, which implies that it is not as reliable as our algorithm. The boxplots medians ignore these awful results, that is why PARE is better than ours in the median. In general, our method does not have flawed executions, and the error is relatively small, therefore demonstrating great effectiveness.

4.2.2. Occlusion analysis

Next, the method's performances are compared with high levels of occlusion, from 50% to 80%. Lower levels output similar fits since most of the consensus methods yield the same ellipse fitting. Thus, in order to carry out this comparison, 1000 runs were computed, and their respective performance profiles were built. The occluded points were generated by the definition of a starting angle $\theta_s \sim U(-\pi, \pi)$, and an ending angle computed as $\theta_e = \theta_s + O_l \cdot 2\pi$, being O_l

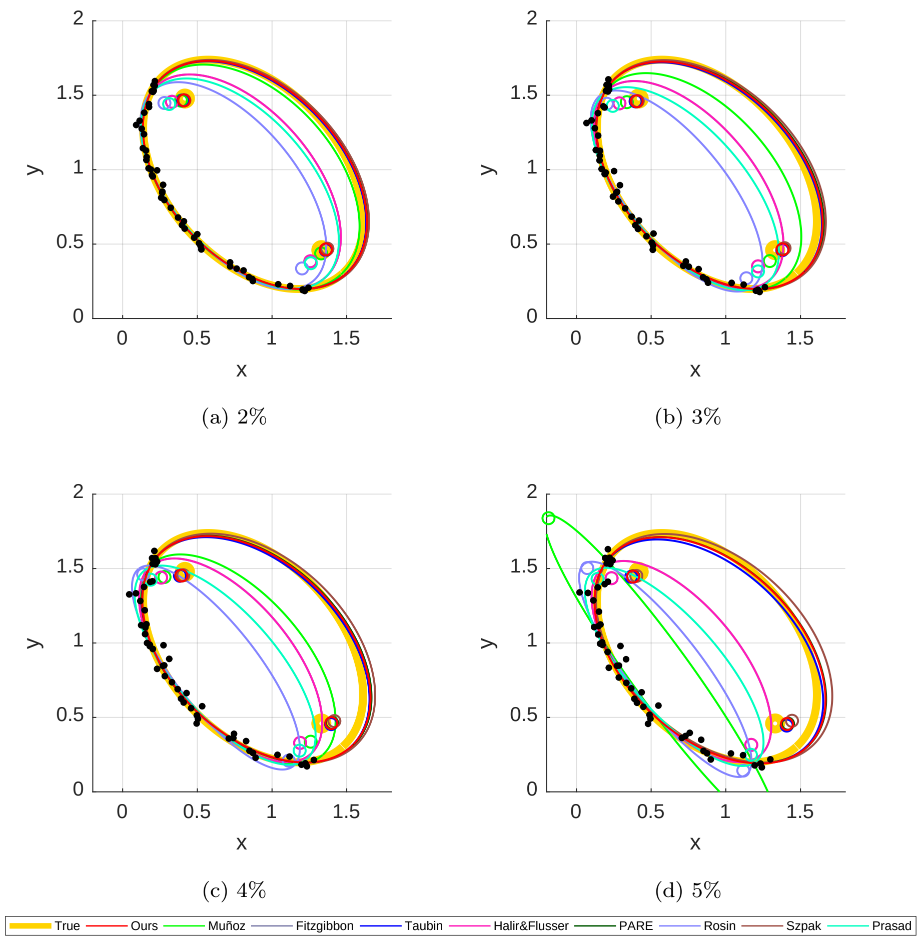

Figure 4: Noise analysis example: outcomes for a particular synthetic dataset modified with 2%, 3% ,4% and 5% of Gaussian noise. The black points are the training samples. The yellow thick curve represents the true ellipse, while the narrow curves show the outcome of each method.

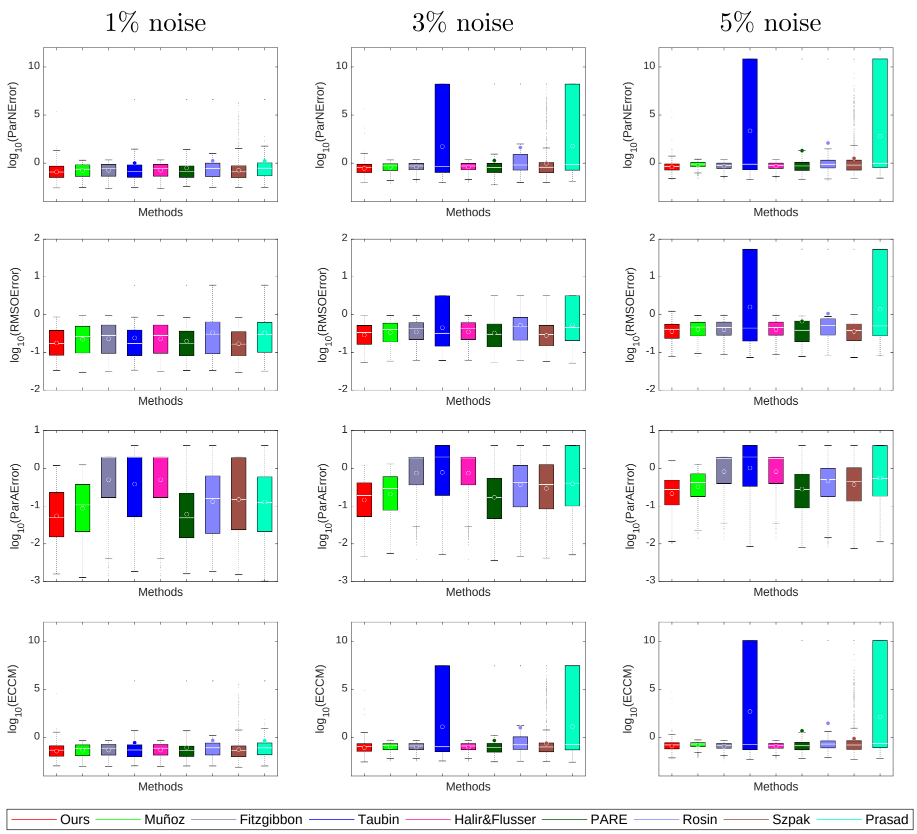

Figure 5: Boxplots of the 1000 runs varying the level of noise. The four error measures are analyzed with 1%, 3%, and 5% of Gaussian noise. Results are shown in a logarithmic scale. Those uncompleted fits were assigned an error equal to twice the maximum error found in the whole set of experiments.

the occlusion level in the range $[0, 1]$. 1% of Gaussian noise was added to the points as explained in previous experiments.

Figure 6 shows the results of the analysis. First, the increase of the level of occlusion generates a larger error, which is normal behavior. If only half of the samples are present, or even at 60% of occlusion, the performance of all methods is quite similar. Specifically, PARE, Szpak, and Taubin methods became very competitive. Furthermore, others like Muñoz and Halir&Flusser yielded bad fits. Recall that Muñoz method was one of the best ellipse fitting methods, as the previous experiments showed, but its bad performance now has not affected the final output of our proposal. That is to say, the proposed method is valid in different fitting problems.

On the other hand, when the level of occlusion is quite high, Muñoz and Szpak methods are the most competitive, raising the performance of our method, as the algebraic, natural, and ECCM error measures have shown while there were more fitting problems that could not be solved. The RMSOError revealed that Ours is the second best, which may be caused by the PARE method's worse performance. Nevertheless, our method is the first one that achieved the best fits of all the runs.

4.3. Bitmap image data

In addition to the synthetic experiments, the performance of our method was assessed evaluating some bitmap image dataset examples. We have selected a total of 12 images: 4 from the Caltech 256 dataset [16], numbered as *137_0008*, *169_0015*, *177_0029* and *216_0011*, other 5 images of wheels that we have captured ourselves, the image of a plate (*Hda_obj93*) from the LabelMe dataset [40], and 2 images of Saturn extracted from the ESA (*Saturn*) and the NASA Voyager (*Saturn rings*) webpages[2]. A total of 20 or 50 points (the latter are for

[2] `https://www.esa.int/Science_Exploration/Space_Science/Cassini-Huygens/The_temperature_of_Saturn_s_rings`, `https://voyager.jpl.nasa.gov/galleries/images-voyager-took/saturn/` (accessed on 30/12/2020)

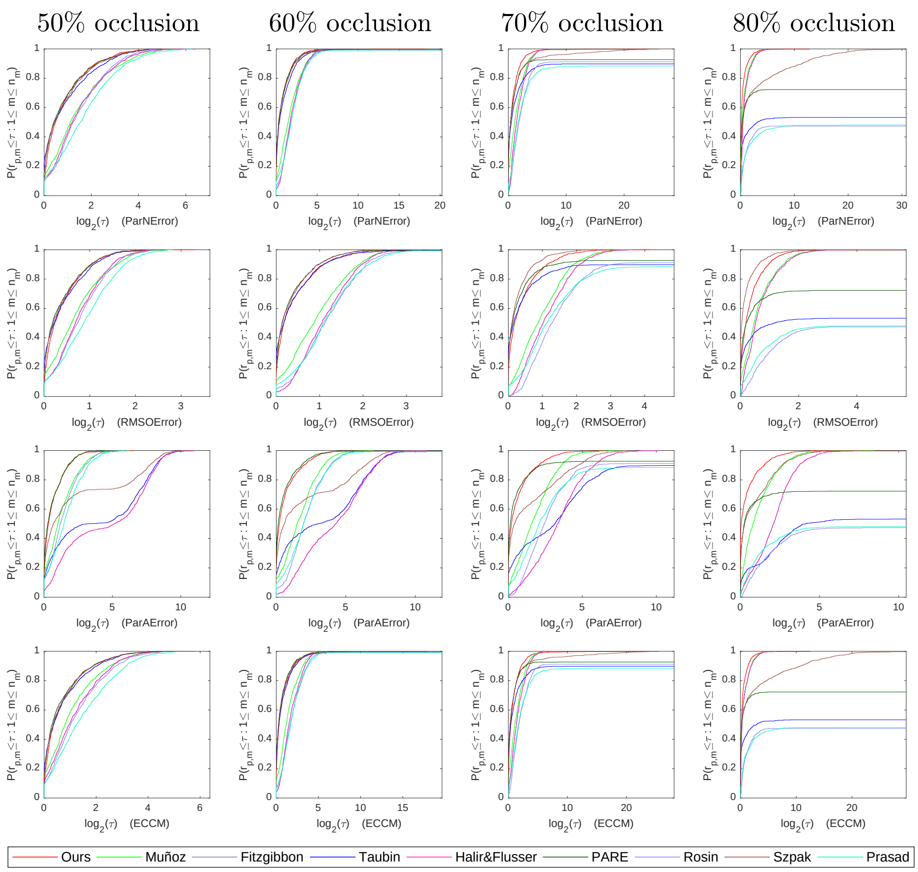

Figure 6: Performance profiles of the 1000 runs varying the level of noise. The four error measures (rows) are analyzed with 50%, 60%, 70%, and 80% of occlusion (columns). Results are shown in a logarithmic scale.

Saturn rings and wheels) were extracted around the ellipse of the figure using the Canny edge detector algorithm, varying its threshold parameter. A single channel image was used, either computing the mean value of the RGB channels or using the Hue channel of the HSV color model, and after the edge detection, the images were refined using morphological functions such as binarizing, filling, border cleaning, and perimeter delimitation. Then, the 20 (or 50) points were selected randomly for each one of the processed images and marked in yellow in the following examples. The point extraction procedure could be replaced by another one since it is not a part of our ellipse fitting method.

In Figure 7 four examples of the execution of the ellipse fitting algorithms are presented. First, a satellite dish in perspective is shown along with its associated fits obtained using all the methods. Here, the major axis and one of the foci are the varying parameters of the resulting fits. Nevertheless, there are no significant differences among algorithms, i.e. all of them fit the ellipse appropriately. One of the five car wheels is also presented. In this case, the edge detection did not achieve a perfect result of the hubcap border, so some outliers are present in the sample dataset. These anomalous points have provoked some disparity among methods. Muñoz and Szpak methods yield a good outcome since they pass through most of the sample points. Our proposal is also one of the best ones, while the others fail in terms of orientation due to the three points that belong to the wheel border. The Saturn image contains three outlying points in the inferior part of the arc, which destabilizes most of the fitting methods (three of them did not give an output). Nevertheless, the spatial median computed by our method maintained the shape of the ring very well. The fourth image corresponds to the *Hda_ obj93* image, whose extraction of points was very noisy. Muñoz, which typically is one of the best methods, and Szpak, failed in the fit but Ours was not affected, being the closer fit to the shape of the plate.

A final example is shown in 8a, where the fitted ellipse was placed overlapping the image for the sake of clarity. This point set is wider and forms two separated noisy groups. The intention was to extract points from the border of the two yellow tones. The fitting methods yield good ellipses, although the clos-

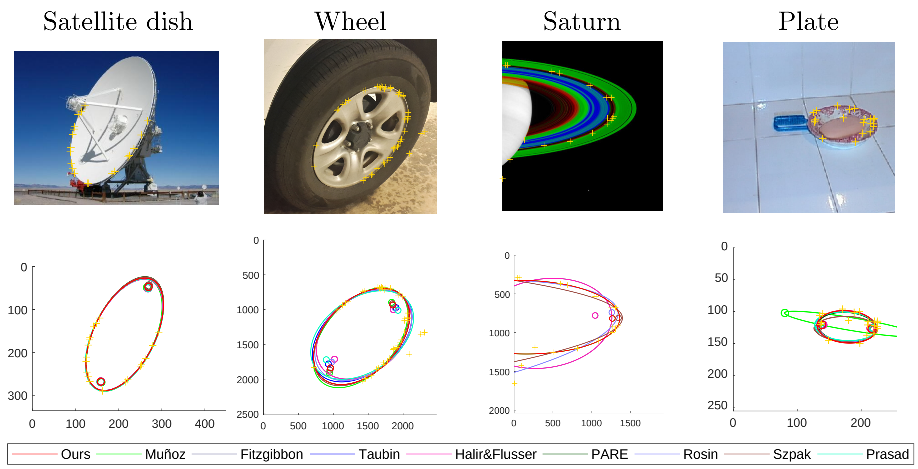

Figure 7: Example of the outcomes for a satellite dish (image *169_0015*), a wheel, the planet Saturn, and a dish plate (image *Hda_obj93*). Points (shown in yellow) were automatically selected using Canny edge detector algorithm. For the sake of clarity, the Y scale of the results was reversed in order to match the original image.

est approximation to the mentioned border are Taubin and Ours, respectively. Finally, in order to have a general overview of our proposal performance compared with the other methods, a rank adjusted for ties to classify each method using the twelve bitmap images was computed. First of all, five true points were manually selected on the shape of the ground truth figure. This was done using the *Ellipse Labeling Tool*[3]. Then, the validity of these point samples was ensured by solving Eq. (8) and overlaying the ellipse on the ground truth image. After that, the same $T = 1000$ test points were generated to compute the RMSO error for each method. Finally, this procedure was repeated for each image and measures were taken to calculate the ranking. The best method achieves one point, the second best method 2 points, and so. For those methods who do not achieve to fit an ellipse, the mean value of the remaining rank points is calculated and assigned to them.

The results of this analysis is depicted in Figure 8b. There are two different

[3]https://sites.google.com/site/dilipprasad/Source-codes (accessed on 04/12/2018)

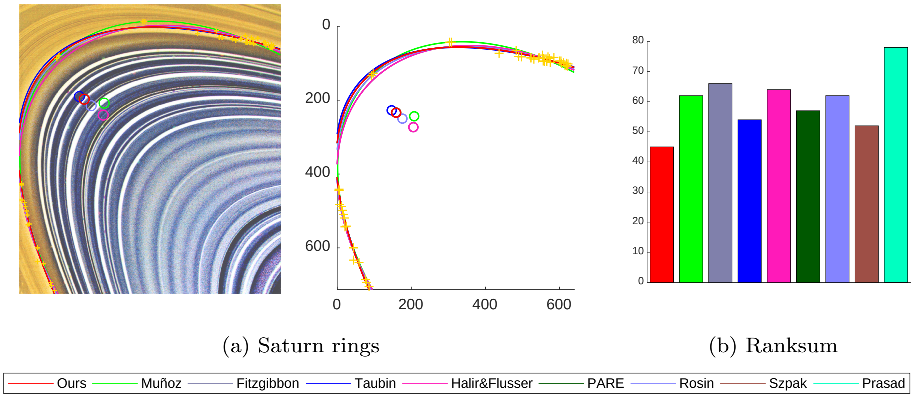

(a) Saturn rings (b) Ranksum

Figure 8: (a) Fitting results for a an image of the Saturn rings (image '169_0015'). Points (shown in yellow) were automatically selected using Canny edge detector algorithm. (b) Ranking of the tested methods using the bitmap image data. Nine images were feeded to each algorithm and they were ordered based on the RMSOError in order to assign the points (lower is better).

groups of methods. Ours, Muñoz, Taubin, PARE and Szpak methods achieve better performance than Fitzgibbon, Halir&Flusser, Rosin and Prasad methods. Our method achieves 45 points, followed by Szpak with 52 and Taubin with 54. Small differences are caused because some methods work better with some images than with others and vice versa. This fact can be analyzed in Table 1 that contains the RMSO error produced for each bitmap image processed by all the fitting methods. It is clear that our proposal does not always yield the best outcome, but for most cases it is very similar to the desired ellipse, such as the *Hda_obj93* image (Ours is the best), or the *Wheels* 1, and 3 (the second best). There are methods, like Muñoz or Taubin, that generate very good outputs but fail in other examples (*137_0008* and *169_0015*). However, Ours is the one with the smallest standard deviation, which means that the procedure is stable and works well with a large diversity of images.

4.4. Discussion

A set of synthetic and bitmap image experiments have been carried out and its outcomes were analyzed with different measures.

Image	*Ours*	*Muñoz*	*Fitzgibbon*	*Taubin*	*H&F*	*PARE*	*Rosin*	*Szpak*	*Prasad*
137_0008	1.329	1.436	1.384	1.319	1.384	1.328	1.385	1.329	1.413
169_0015	1.997	2.136	2.168	2.000	2.168	1.794	2.061	1.834	2.035
177_0029	5.448	5.272	5.467	5.344	5.467	5.463	5.496	5.452	5.570
216_0011	4.493	3.624	3.270	—	3.270	—	3.515	4.064	—
Wheel 1	2.546	2.188	2.555	2.562	2.555	2.550	2.561	2.559	2.568
Wheel 2	7.579	2.103	9.326	9.569	9.326	5.603	9.329	3.470	9.565
Wheel 3	3.241	3.608	3.231	3.220	3.231	3.243	3.229	3.280	3.217
Wheel 4	1.612	1.798	1.598	1.596	1.598	1.612	1.597	1.619	1.594
Wheel 5	4.862	3.073	7.500	6.423	7.500	4.862	6.833	4.073	7.642
Hda_obj93	3.969	5.010	3.973	4.029	3.973	4.109	4.077	4.376	4.155
Saturn rings	24.580	41.517	41.588	7.558	41.588	24.581	36.238	24.083	31.240
Saturn	18.860	18.860	25.765	—	25.765	—	14.402	15.288	—
Rank mean	**3.750**	5.167	5.500	4.500	5.333	4.750	5.167	4.333	6.500
Rank std	**1.689**	3.387	2.327	2.901	1.886	2.203	2.075	2.461	2.784

Table 1: RMSOError of each bitmap image. Also, mean and standard deviations of the rank points assigned for each method using the bitmap image data is computed. Best results are marked in bold (lower is better).

Regarding synthetic data results, the proposed method is not severely affected by high levels of occlusion, while the other methods yield ellipses with wrong sizes or orientations. First, in terms of the ParN error, our method solves almost 95% of the executions with better error ratio together with Muñoz and Halir&Flusser methods whereas Prasad, PARE, and Taubin fail in 10-20% of the fitting tests. Second, considering the RMSO error, our method follows the Szpak method achieving the second-best place. Therefore, those methods that attain the highest positions for the ParN error do not present good results for the RMSO error and vice versa, except for our proposal, which performs nicely with respect to both performance metrics. In addition, the obtained ParA errors reveal a similar tendency. Here, the PARE method becomes very competitive, although 10% of the fits are not solved and our proposal shares the first position with him. Thus, it remains stable among the first positions in all cases, being the only method that is able to solve all the fits with the lowest error among the three measures.

Consequently, the consensus is more precise than any of the other methods applied separately. In addition, after studying the behavior of our method under a certain level of noise (2%), it clearly outperforms all competing methods in terms of the ParN and ECCM error, while for the RMSO error presents the second-best error ratio for almost all executions, only after Szpak method. Moreover, under higher noise levels (4-5%) Szpak method does not work appropriately even with the ParA error, thus, generating PARE and the proposed method the best ellipses. Also, it is important to remark the good contribution of Muñoz method to the consensus, since it is the most stable algorithm among the rest, also reaching the 100% of the fits. This guarantees that our method is always able to find a solution that is improved by the incorporation of the information generated by the others.

The occlusion experiments also demonstrated the effectiveness of our proposal. In these runs the performance of methods like Muñoz, which worked well before, decreased considerably. Nevertheless, others like PARE, Szpak, or Taubin, supported the spatial median calculation, making our outputs very competitive. Specially when the level of occlusion increased, as the ECCM, ParAError and ParNError reflects.

Finally, as to bitmap image data, our method achieves the smallest standard deviation. Once again, this reveals that the proposed method is the most stable and works well with a wide range of bitmap images. The depicted examples show the difference in performances when higher levels of noise are present in the samples. If the shape of the ellipse is clearly distinguishable, that is, low level of noise is present (e.g., the satellite dish)), the outcomes of all methods are similar. However, when the samples are disturbed considerably, that is, there is a higher level of noise (e.g., the wheel), our method is able to get the best of the fitted parameters of the consensus methods.

From the preceding, it follows that our proposal exhibits a consistently higher performance and lower variability according to the range of tested performance measures across a wide variety of situations. This robustness is due to the appropriate combination of several state-of-art ellipse fitting methods.

5. Conclusions

A consensus method has been developed to fit an elliptical feature to a set of points by combining the estimations obtained by several algorithms. The combination is carried out by computing the L1 median of several components of a natural parametrization of the ellipse, which is particularly suited to this kind of averaging. The rationale of our approach is that if a few methods break down due to the deleterious effect of noise, but the majority of the methods still produce adequate fits, then the computation of the L1 median of the natural parametrizations of the solutions leads to a reasonable fit of the ellipse.

Therefore, our proposal is based on the consensus of many alternative ellipse fits obtained by a base method. It has the novelty that the alternative fits are averaged in a specifically chosen ellipse parameter space where averaging yields more accurate consensus fits, namely the natural parameter space. Moreover, the L1 median has been proposed in order to enhance the performance of the consensus when defective ellipse fits arise. All of these are novel strategies, which have not been considered before in the literature.

The experimental design which has been developed to test the proposal involves the comparison of the competitors to the parameters of the true ellipse with respect to the Root Mean Square Orthogonal error on one side, and building performance profiles of the set of methods on a test set to compare them with the best performance achieved by any of the solvers on this issue on the other side. The synthetic and bitmap image results indicate that our consensus methodology provides great results for all error measures and at any level of noise.

All in all, after the considerations made and the analysis performed, the proposed consensus method is more accurate than the methods which are combined for the consensus. That is, the L1 median calculation over the natural parametrization of the ellipse has been found to be suitable for the aggregation of the results of several ellipse fitting methods. The main strength of our approach is that it compensates any large errors committed by a minority of methods, provided that the majority of the methods still produce acceptable fits. Therefore, the shortcomings of the combined methods for specific input datasets are averaged out in a reliable way.

The ensemble strategy that is advocated in this work has consistently demonstrated that it boosts the performance of the combined methods. This novel strategy has the potential to further enhance the performance of other ellipse fitting methods because it can be applied to any methods developed in the future.

The proposed approach could be extended to other tasks such as parabola or ellipsoid fitting, which are common problems in several applications in medicine or architecture. In these cases, the algorithms to be combined should be chosen carefully so that they usually produce good approximations to the shape to be estimated. However, the theoretical framework of our proposed method should be similar.

Acknowledgments

This work is partially supported by the Ministry of Economy and Competitiveness of Spain [grant numbers TIN2016-75097-P and PPIT.UMA.B1.2017]. It is also partially supported by the Ministry of Science, Innovation and Universities of Spain [grant number RTI2018-094645-B-I00], project name Automated detection with low-cost hardware of unusual activities in video sequences. It is also partially supported by the Autonomous Government of Andalusia (Spain) under project UMA18-FEDERJA-084, project name Detection of anomalous behavior agents by deep learning in low-cost video surveillance intelligent systems. All of them include funds from the European Regional Development Fund (ERDF). The authors thankfully acknowledge the computer resources, technical expertise and assistance provided by the SCBI (Supercomputing and Bioinformatics) center of the University of Málaga. They also gratefully acknowledge the support of NVIDIA Corporation with the donation of two Titan X GPUs. The authors acknowledge the funding from the Universidad de

Málaga. Karl Thurnhofer-Hemsi is funded by a Ph.D. scholarship from the Spanish Ministry of Education, Culture and Sport under the FPU program [grant number FPU15/06512]. Funding for open access charge: Universidad de Málaga / CBUA.

References

[1] S. Ahn, W. Rauh, H.-J. Warnecke, Least-squares orthogonal distances fitting of circle, sphere, elipse, hyperbola, and parabola, Pattern Recognition 34 (12) (2001) 2283–2303.

[2] A. R. Backes, O. M. Bruno, Polygonal approximation of digital planar curves through vertex betweenness, Information Sciences 222 (2013) 795 – 804.

[3] G. Beliakov, S. James, T. Wilkin, Aggregation and consensus for preference relations based on fuzzy partial orders, Fuzzy Optimization and Decision Making 16 (4) (2017) 409–428.

[4] V. Bolón-Canedo, A. Alonso-Betanzos, Ensembles for feature selection: A review and future trends, Information Fusion 52 (2019) 1 – 12.

[5] F. Cabrerizo, F. Chiclana, R. Al-Hmouz, A. Morfeq, A. Balamash, E. Herrera-Viedma, Fuzzy decision making and consensus: Challenges, Journal of Intelligent and Fuzzy Systems 29 (3) (2015) 1109–1118.

[6] H. I. Cakir, C. Topal, An euclidean ellipse comparison metric for quantitative evaluation, in: IEEE International Conference on Acoustics, Speech and Signal Processing (ICASSP), 1263–1267, 2018.

[7] G. Calafiore, Outliers robustness in multivariate orthogonal regression, IEEE Transactions on Systems, Man, and Cybernetics Part A: Systems and Humans 30 (6) (2000) 674–679.

[8] G. Calafiore, Approximation of n-dimensional data using spherical and ellipsoidal primitives, IEEE Transactions on Systems, Man, and Cybernetics Part A: Systems and Humans 32 (2) (2002) 269–278.

[9] W. Chojnacki, M. Brooks, A. Vanel, On the fitting of surfaces to data with covariances, IEEE Transactions on Pattern Analysis and Machine Intelligence 22 (11) (2000) 1294–1303.

[10] L. De La Fraga, I. Silva, N. Cruz-Cortes, Euclidean distance fit of ellipses with a genetic algorithm, in: Lecture Notes in Computer Science (including subseries Lecture Notes in Artificial Intelligence and Lecture Notes in Bioinformatics), vol. 4448 LNCS, 359–366, 2007.

[11] T. G. Dietterich, Ensemble Methods in Machine Learning, in: Multiple Classifier Systems, Springer Berlin Heidelberg, Berlin, Heidelberg, ISBN 978-3-540-45014-6, 1–15, 2000.

[12] E. D. Dolan, J. J. Moré, Benchmarking optimization software with performance profiles, Mathematical Programming 91 (2) (2002) 201–213.

[13] Y. Dong, X. Chen, F. Herrera, Minimizing adjusted simple terms in the consensus reaching process with hesitant linguistic assessments in group decision making, Information Sciences 297 (2015) 95–117.

[14] A. Fitzgibbon, R. Fisher, A buyer's guide to conic fitting, British Machine Vision Conference (1995) 513–522.

[15] A. Fitzgibbon, M. Pilu, R. Fisher, Direct least squares fitting of ellipses, IEEE Trans. Pattern Analysis and Machine Intelligence 21 (5) (1999) 476–480.

[16] G. Griffin, A. Holub, P. Perona, Caltech-256 Object Category Dataset, CalTech Report .

[17] R. Halir, J. Flusser, Numerically stable direct least squares fitting of ellipses, The Sixth International Conference in Central Europe on Computer Graphics and Visualization (1998) 125–132.

[18] E. Herrera-Viedma, F. J. Cabrerizo, J. Kacprzyk, W. Pedrycz, A review of soft consensus models in a fuzzy environment, Information Fusion 17 (2014) 4 – 13, Special Issue: Information fusion in consensus and decision making.

[19] O. Hössjer, C. Croux, Generalizing univariate signed rank statistics for testing and estimating a multivariate location parameter, Journal of Nonparametric Statistics 4 (3) (1995) 293–308.

[20] M. T. Islam, E. Tasciotti, R. Righetti, Estimation of Vascular Permeability in Irregularly Shaped Cancers Using Ultrasound Poroelastography, IEEE Transactions on Biomedical Engineering 67 (4) (2020) 1083–1096.

[21] K. Kanatani, Statistical Bias of Conic Fitting and Renormalization, IEEE Transactions on Pattern Analysis and Machine Intelligence 16 (3) (1994) 320–326.

[22] K. Kanatani, Y. Sugaya, Unified computation of strict maximum likelihood for geometric fitting, Journal of Mathematical Imaging and Vision 38 (1) (2010) 1–13.

[23] J. T. Kent, F. Er, P. D. L. Constable, Algorithms for the Spatial Median, in: K. Nordhausen, S. Taskinen (Eds.), Modern Nonparametric, Robust and Multivariate Methods: Festschrift in Honour of Hannu Oja, Springer International Publishing, ISBN 978-3-319-22404-6, 205–224, 2015.

[24] A. Kozierkiewicz-Hetmańska, The analysis of expert opinions' consensus quality, Information Fusion 34 (2017) 80 – 86.

[25] Y. Leedan, P. Meer, Heteroscedastic regression in computer vision: problems with bilinear constraint, International Journal of Computer Vision 37 (2) (2000) 127–150.

[26] H. Li, Multiple ellipse fitting of densely connected contours, Information Sciences 502 (2019) 330 – 345.

[27] X. Liu, Y. Xu, F. Herrera, Consensus model for large-scale group decision making based on fuzzy preference relation with self-confidence: Detecting and managing overconfidence behaviors, Information Fusion 52 (2019) 245 – 256.

[28] E. López-Rubio, K. Thurnhofer-Hemsi, E. B. Blázquez-Parra, O. D. de Cózar-Macías, M. C. Ladrón-de Guevara-Muñoz, A fast robust geometric fitting method for parabolic curves, Pattern Recognition 84 (2018) 301 – 316.

[29] B. Matei, P. Meer, Estimation of nonlinear errors-in-variables models for computer vision applications, IEEE Transactions on Pattern Analysis and Machine Intelligence 28 (10) (2006) 1537–1552.

[30] P. Meer, D. Mintz, A. Rosenfeld, D. Kim, Robust regression methods for computer vision: A review, International Journal of Computer Vision 6 (1) (1991) 59–70.

[31] J. Mottonen, K. Nordhausen, H. Oja, Asymptotic theory of the spatial median, in: J. Antoch, M. Huskova, P. Sen (Eds.), Nonparametrics and Robustness in Modern Statistical Inference and Time Series Analysis: a Festschrift in Honor of Professor Jana Jureková, Institute of Mathematical Statistics, Beachwood, Ohio, USA, ISBN 978-3-642-35494-6, 182–193, 2010.

[32] J. Moyano, E. Gibaja, K. Cios, S. Ventura, Review of ensembles of multi-label classifiers: Models, experimental study and prospects, Information Fusion 44 (2018) 33–45.

[33] J. Muñoz-Pérez, O. D. de Cózar-Macías, E. B. Blázquez-Parra, I. Ladrón de Guevara-López, Multicriteria Robust Fitting of Elliptical Primitives, J Math Imaging Vis 49 (2014) 492–509.

[34] H. Oja, Multivariate Median, in: C. Becker, R. Fried, S. Kuhnt (Eds.), Robustness and Complex Data Structures: Festschrift in Honour of Ursula

Gather, Springer Berlin Heidelberg, Berlin, Heidelberg, ISBN 978-3-642-35494-6, 3–15, 2013.

[35] R. Pérez-Fernández, M. Sader, B. D. Baets, Joint consensus evaluation of multiple objects on an ordinal scale: An approach driven by monotonicity, Information Fusion 42 (2018) 64 – 74.

[36] D. Prasad, M. Leung, C. Quek, ElliFit: An unconstrained, non-iterative, least squares based geometric Ellipse Fitting method, Pattern Recognition 46 (5) (2013) 1449–1465.

[37] A. Ray, D. Srivastava, Non-linear least squares ellipse fitting using the genetic algorithm with applications to strain analysis, Journal of Structural Geology 30 (12) (2008) 1593–1602.

[38] P. Rosin, Further five-point fit ellipse fitting, Graphical Models and Image Processing 61 (5) (1999) 245–259.

[39] G. Roth, M. Levine, Extracting geometric primitives, Computer Vision and Image Understanding 58 (1) (1993) 1–22.

[40] B. C. Russell, A. Torralba, K. P. Murphy, W. T. Freeman, LabelMe: a database and web-based tool for image annotation, International journal of computer vision 77 (1-3) (2008) 157–173.

[41] P. Sampson, Fitting conic sections to very scattered data: An iterative refinement of the bookstein algorithm, Computer Graphics and Image Processing 18 (1) (1982) 97–108.

[42] Z. Szpak, W. Chojnacki, A. van den Hengel, Guaranteed Ellipse Fitting with a Confidence Region and an Uncertainty Measure for Centre, Axes, and Orientation, Journal of Mathematical Imaging and Vision 52 (2) (2015) 173–199.

[43] G. Taubin, Estimation of Planar Curves, Surfaces, and Nonplanar Space Curves Defined by Implicit Equations with Applications to Edge and Range

Image Segmentation, IEEE Transactions on Pattern Analysis and Machine Intelligence 13 (11) (1991) 1115–1138.

[44] E. Ülker, A. Arslan, Automatic knot adjustment using an artificial immune system for B-spline curve approximation, Information Sciences 179 (10) (2009) 1483 – 1494.

[45] R. Usamentiaga, D. Garcia, Multi-camera calibration for accurate geometric measurements in industrial environments, Measurement: Journal of the International Measurement Confederation 134 (2019) 345–358.

[46] Z. Wu, J. Xu, A consensus model for large-scale group decision making with hesitant fuzzy information and changeable clusters, Information Fusion 41 (2018) 217–231.

[47] J. Yu, S. Kulkarni, H. Poor, Robust ellipse and spheroid fitting, Pattern Recognition Letters 33 (5) (2012) 492–499.

[48] Y. Zhang, Y. Li, B. Xie, X. Li, J. Zhu, Pupil localization algorithm combining convex area voting and model constraint, Pattern Recognition and Image Analysis 27 (4) (2017) 846–854.

[49] Z. Zhang, Parameter estimation techniques: a tutorial with application to conic fitting, Image and Vision Computing 15 (1) (1997) 59–76.